Annual Performance Report

(1 July 1991 through 30 June 1992)

Grant Title: Electro-Rheology Fluids and Liquid Fuel Flow

Grant NO: N00014-90-J-4041

R&T Number: 4329474—01

Scientific Officer: Dr. Gabriel D. Roy, Office of Naval Research

Principal Investigator: Dr. Rongjia Tao

Mailing Address: Department of Physics, Southern Illinois University, Carbondale, IL 62901

Phone number: (618)-536-2117, **Fax:** (618)-453-8216

E-Mail Address: GA3756@SIUCVMB.SIU.EDU

Co-PI of the Grant: Dr. Robert N. Zitter

Post-Docs Supported on the Grant: Dr. Tian-Jie Chen, Dr. Xuesong Zhang, and Dr. Qi Jiang

Graduate Students Supported on the Grant: Mr. Gerald Gulley and J. M. Sun

I. Scientific Research Goals

The goals of this research are

- to understand and clarify the physical mechanism underlying the electrorheological (ER) response of fluids and establish a theory for the phenomenon;
- to study the structure of ER fluids and their properties, to investigate the change of viscosity of ER fluids with an applied electric field;
- to apply the ER phenomenon to liquid fuel flows, to control their viscosity and hence their velocity;
- to examine the necessary theoretical and technique problems associated to the design of a new class of liquid fuel control devices which are based on the ER phenomenon.

II. Significant Results in the Past Year

Our research in this period has made significant progress toward the above goals.

1. Determination of the induced ER structure by laser diffraction

The structure of ER fluids in an electric field is an important issue to understand the ER phenomenon. Our theoretical work last year predicted that the induced ER solid has an ideal structure of a body-centered tetragonal (bct) lattice structure, as illustrated in Fig.1(a).* The three conventional lattice vectors are $\sqrt{6}R\hat{x}$, $\sqrt{6}R\hat{y}$, and $2R\hat{z}$, with the field along the z direction.

The prediction of a bct lattice as a many-body ground state of ER fluids has been confirmed by our Monte Carlo simulations, which have also shown that this structure can be realized at room temperature.† However, there has been no experimental verification of the structure. Since the electric field-induced solidification in ER fluids is a relatively fast phase transition, it would be interesting to see if a regular lattice can be formed in the process. Furthermore, most existing theoretical models and calculations of ER fluid properties assume particles in chains rather than columns. Therefore, an experimental determination of column structure would be highly significant for future research and applications.

We have used laser beam diffraction to investigate the structure of induced ER solid, which confirms the predicted bct lattice structure. The diffraction mechanism, however, is totally unlike that of conventional X-ray scattering by crystals.

Our ER fluid consists of a low viscosity silicone oil containing size-selected glass micro-spheres of highly uniform diameter, either 20.0 ± 1.8 μm or 40.7 ± 1.7 μm (SPI Supplies, Westchester, PA). The glass spheres were pre-treated to develop an absorbed H_2O film which greatly enhances their effective dielectric constant, and then the spheres were mixed with oil to a volume fraction about 0.2. On a horizontal microscope glass slide we mounted two parallel brass electrodes which are 3 mm thick and separated by 3 mm. Then three glass spacers were used between the electrodes, one at the bottom, two at the two sides, to form an ER fluid cell in a region of most uniform electric field. Only a small drop of the ER liquid is needed to fill the cell, measuring 3 mm × 3 mm horizontally and 0.3 mm in vertical depth. The top surface of the fluid is open (no cover glass is

* R. Tao and J. M. Sun, Phys. Rev. Lett. 67, 398 (1991).
† R. Tao and J. M. Sun, Phys. Rev. A., 44, R6181 (1991).

used). Before an electric field was applied, the spheres stayed at the bottom and formed several layers. We stirred the ER fluid in the cell first to make the spheres spread into the space, then we began to apply an electric field. The solidification process takes about 5 minutes and is recorded by a video camcorder, showing the formation of chains then columns for applied electric fields $\sim$ 1 KV/mm. If the field is maintained for several hours, the oil leaks out of the cell, the structures become "locked" in place, remaining fixed after removal of the field. The averaging column width is 0.6 mm. The column thickness vertical to the slide is about 0.15 mm. The average separation between two columns is generally several column widths.

The diffraction of a laser beam by glass spheres in a closed-packed lattice such as that shown in Fig. 1(a) needs to be carefully examined. It certainly is *not* analogous to conventional X-ray diffraction by a crystal. For X-rays, a crystal is essentially transparent with a 3-dimensional array of small scattering centers (nuclei and electrons) that produce far-field interference patterns. In our ER structure, the glass spheres have a size much larger than the laser wavelength (0.63 μm), and the closely packed structure is "optically dense" in the sense that there are very few paths for light to travel without encountering a number of spheres. In fact, for example, there is no direct path in the [110] direction. Although one might expect diffuse scattering of a laser beam due to multiple reflections and refractions by the spheres, a mechanism for producing regular patterns is not immediately obvious.

We have proposed the following process. Since each glass sphere acts as a "thick" lens, a linear periodically spaced set of spheres, as shown in Fig.1(b), constitutes a periodic array of focussing elements. An analysis of such arrays can be found in many texts, where it is shown that light rays can propagate stably and indefinitely along an appropriately spaced set of such elements. In other words, there are stable ray modes that do not diverge from the axis, or leave the array. This analysis is often employed in laser design, where an infinite array is used to represent the end-reflectors of an optical cavity. Mathematically, the path of a ray along a single periodic length is characterized by a 2×2 matrix M, and stable ray modes exist if the absolute value of the trace of M is less than 2.

The calculation of M is simple for "paraxial" rays close to the array axis that make only small angles from the axis. For the array represented in Fig.1(b), the matrix for the period from the front surface of one sphere to the front surface of the next is given by

$$M = \begin{pmatrix} 1 & d \\ 0 & 1 \end{pmatrix} \begin{pmatrix} 1 & 0 \\ (1-n)/R & n \end{pmatrix} \begin{pmatrix} 1 & 2R \\ 0 & 1 \end{pmatrix} \begin{pmatrix} 1 & 0 \\ (1-n)/nR & 1/n \end{pmatrix}$$

$$= \begin{pmatrix} [(2-n)/n] + [2d(1-n)/nR] & [2R/n] + [d(2-n)/n] \\ 2(1-n)/nR & (2-n)/n \end{pmatrix} \qquad (1)$$

where R is the radius, n is the ratio of the refractive index of the spheres to the refractive index of air medium, and the matrices in the product, reading from right to left, represent respectively (i) refraction entering a sphere, (ii) traverse through the sphere, (iii) refraction leaving the sphere, and (iv) traverse of the space d between two spheres. Each of these matrices can be found in the ray-matrix tables.* For stable ray modes, the absolute value of the trace of M must be less than 2. Then, from Eq.(1), we obtain the stability condition

$$d < 2R/(n-1). \qquad (2)$$

Our samples, after the oil leaks out, have $n = n_{glass}/n_{air} = 1.51$ and thus we require $d < 3.9R$ for stable mode propagation. For the bct lattice shown in Fig. 1(a), all directions $[m, n, l]$ with low indices $(m, n, l = 0, \pm 1)$ satisfy the above condition, and accordingly, stable paraxial ray modes may propagate along these directions. More extensive calculations show that stable non-paraxial modes may also propagate in the bct lattice.

Thus, stable modes travel along each linear array and emerge from the final sphere to a focus beyond the last lattice plane. The focal waist size is only a few micrometers in diameter, small in comparison with the sphere radius. The set of such focal "points" is essentially a 2-dimensional array (not 3-dimensional as in

* See, for example, A. E. Siegman, *Lasers* (University Science Books, Mill Valley CA,1986), Chap.15.

X-rays) that produces a diffraction pattern. The form of the far-field diffraction pattern is just the reciprocal lattice of the exit plane.

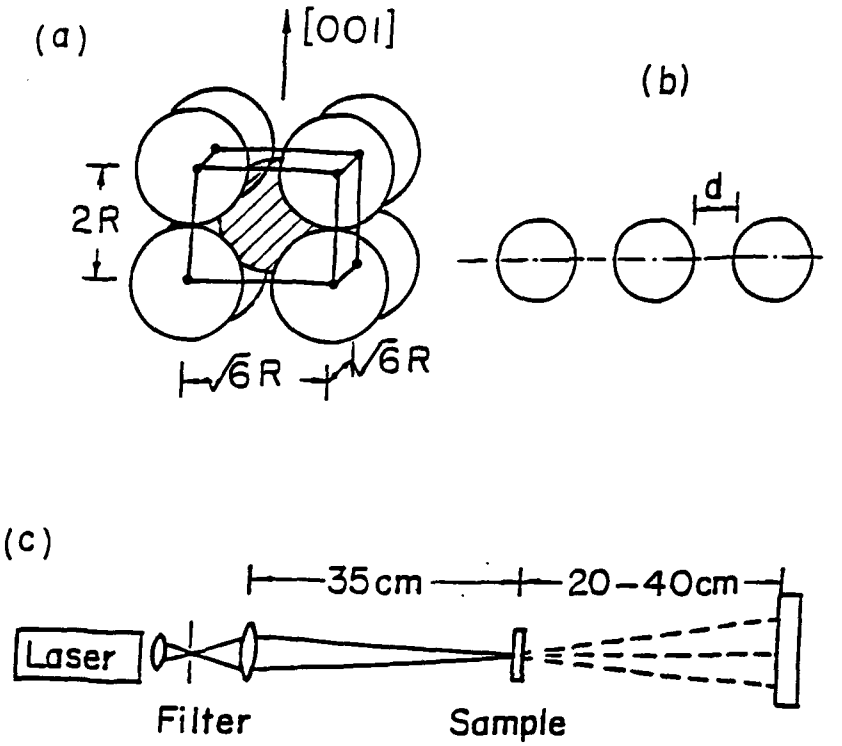

Fig.1. (a) Unit cell of our proposed bct lattice for spheres of radius R, where the [001] axis is the applied field direction. (b) A linear periodic array of glass spheres of radius R separated by distance d. (c) Layout of the diffraction experiment. In the sample, whose view is given in Fig.2(a), the applied electric field direction [001] is perpendicular to the optic axis.

The experimental optical diffraction arrangement is shown in Fig.1(c). A 5mw He-Ne laser beam is passed through a spatial pinhole filter to obtain a clean Gaussian intensity profile and then is focused onto an individual column of the sample. The focused laser beam has a Gaussian diameter about 0.1 mm or 1/6 of the average column width. The sample is on a micrometer adjustable mount for translation and angular rotation. We note a fundamental difference between our experiment and conventional X-ray diffraction by a crystal. In the latter case,

the Bragg condition requires a specific orientation of the incident beam relative to crystal planes, and all orientations must be used to obtain a complete pattern. By contrast, our experiment is insensitive to the incident beam direction and an entire planar pattern for the lattice exit plane is obtained for a single orientation of the sample relative to the incident beam. This is because each sphere in the first layer encountered by the beam produces refracted rays in various directions, from which propagating array modes are selected by deeper-lying layers.

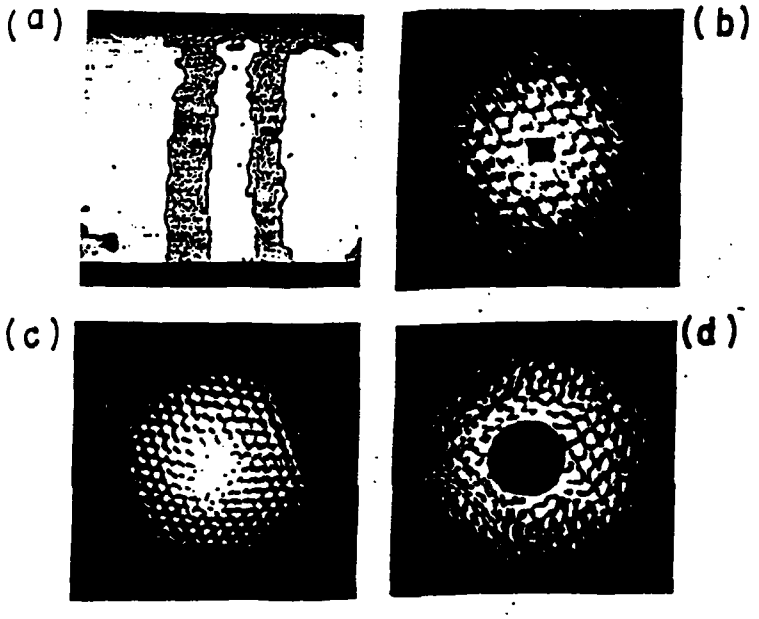

Fig.2. (a) View of typical columns formed between the two electrodes which are separated by 3mm. (b) Diffraction pattern of a (110) plane for 20.0 μm diameter spheres. (c) Pattern of a (110) plane for 40.7 μm diameter spheres. (d) Pattern of a (100) plane for 40.7 μm diameter spheres. In (b) and (d), the centers are masked to suppress overexposure.

The bct lattice structure can be identified by the structures of the (110) and (100) planes. The (100) plane has a rectangle $\sqrt{6}R \times 2R$ as a primitive cell, while the (110) plane is a centered rectangular lattice of $2\sqrt{3}R \times 2R$. Fig.2(a) is a microscopic view of typical columns. Fig.2(b) shows a diffraction pattern produced by a sample with 20.0 μm diameter spheres. The geometry of this pattern is precisely the reciprocal lattice of the (110) plane in the bct structure

and the structure constants derived from the pattern are precisely those expected for this plane. This implies that the transmission axis of stable ray modes is along axis [110]. Fig.2(c) shows a pattern from a sample with 40.7 μm diameter spheres. Here the pattern is also that of a reciprocal lattice of the (110) plane, but twice as dense as in Fig.2(b) because with spheres twice as large the reciprocal spacing is smaller by 1/2. In Fig.2(d), the sphere diameter is 40.7 μm and the pattern is obviously more rectangular than the preceding cases; it is in fact, precisely the pattern expected for a (100) plane. In this case, the transmission axis of stable ray modes is [100]. The direction [010] is equivalent to [100] in the bct structure. All of our samples have shown the diffraction patterns consistent with the bct lattice structure.

Table I lists experimental results of the structure constants compared with theoretical values for the bct lattice. In all cases, there is agreement to within a few percent. As mentioned earlier, the diameters of our spheres are known to be non-uniform to this degree. Accordingly, the data are entirely consistent with the proposed bct lattice.

Table I. Structure constants

Lattice Plane	Sphere Diameter	Experiment	Theory
(110)	20.0 μm	$a = 34.1$ μm	34.6 μm
		$b = 21.1$ μm	20.0 μm
(110)	40.7 μm	$a = 69.1$ μm	70.5 μm
		$b = 38.9$ μm	40.7 μm
(100)	40.7 μm	$a = 54.8$ μm	49.8 μm
		$b = 43.8$ μm	40.7 μm

2. Theoretical study of the viscosity as a function of field

In an electric field, the apparent viscosity of ER fluids increases dramatically. It is very important to understand the mechanism of this phenomenon and characterize the relationship between the applied electric field and the viscosity.

We are studying a model which has fine dielectric spheres in a liquid. The particle density in the system is low. The liquid and the particles are flowing through a parallel capacitor. The electric field inside the capacitor induces formation of chains between two plates. If the liquid has viscosity η, there is a drag force acting on the particle, $6\pi\eta av$, where a is the particle radius, v is the relative velocity of the liquid to the particle. This drag force bends the chains. We are calculating the shape of the chains as a function of the strength of electric field and the flow velocity. Hence, we calculate the change of apparent viscosity and connect the present problem to the well-studied problem of flow in porous media.

We have obtained some interesting results. There is a dimensionless quantity $\lambda = \eta v a^5/p^2$ which marks the ratio between the flow drag force and the dipolar force. First, when the flow velocity is not too high, the shape of a chain can be described by an equation, $y = c_1 - c_2 x^2 + c_3 x^4$, where the flow is in the $y-$direction and the electric field in the $x-$direction. The origin of the coordinate is at the middle between the two parallel plates. The constants c_1, c_2, and c_3 are determined by balance of all forces on a particle and found to be functions of λ. However, as the flow velocity gets too high, the chains begin to break. Therefore, there is a critical value of λ . As λ is greater than this critical value, the chain cannot hold in the flow. We have also found that the average viscosity increases in the form $\exp(\alpha E^2)$ where α is a constant.

3. Experimental measurements of the viscosity

The ER suspension in our experiment has pump oil (viscosity, $\eta = 0.0705$ poise) and silica gel particles which have diameters, varying between $106\mu m$ and $185\mu m$, with an average 145μm. The fluid is flowing through a chamber which is defined as the y axis. The cross-section of the chamber is $6mm \times 6mm$. The gel particles are dyed in blue for a better observation. We have found that the flow rate is reducing dramatically as the applied field increases. At a volume fraction about 5%, a moderate electric field, the flow is completely stopped. From the flow rate, we calculate the apparent viscosity which is shown in Fig.3.

We have paid a special attention to the chain shape in the flow. In order to observe a thin chain, we keep the particle number density in the suspension low. A static electric field of $E = 15.66KV/cm$ is applied in the x direction.

The profile of the chain is enlarged through an optical system and recorded by a camera. The chain can be fitted by a polynomial $y = -ax^2 + bx^4$ where the field in the $x-$direction and the origin of the coordinate is at the middle between the two parallel plates. When the average flow rate is $v_{ave} = 0.417 cm/sec$, for example, the polynomial has $a = 0.4617$ and $b = 0.1579$. The computer calculation, based on dipolar interaction, finds the same shape curve with $a = 0.278$ and $b = 0.056$. The match is reasonably good, but the difference is not negligible. We consider that the main difference is due to dipole approximation. A further study is under way.

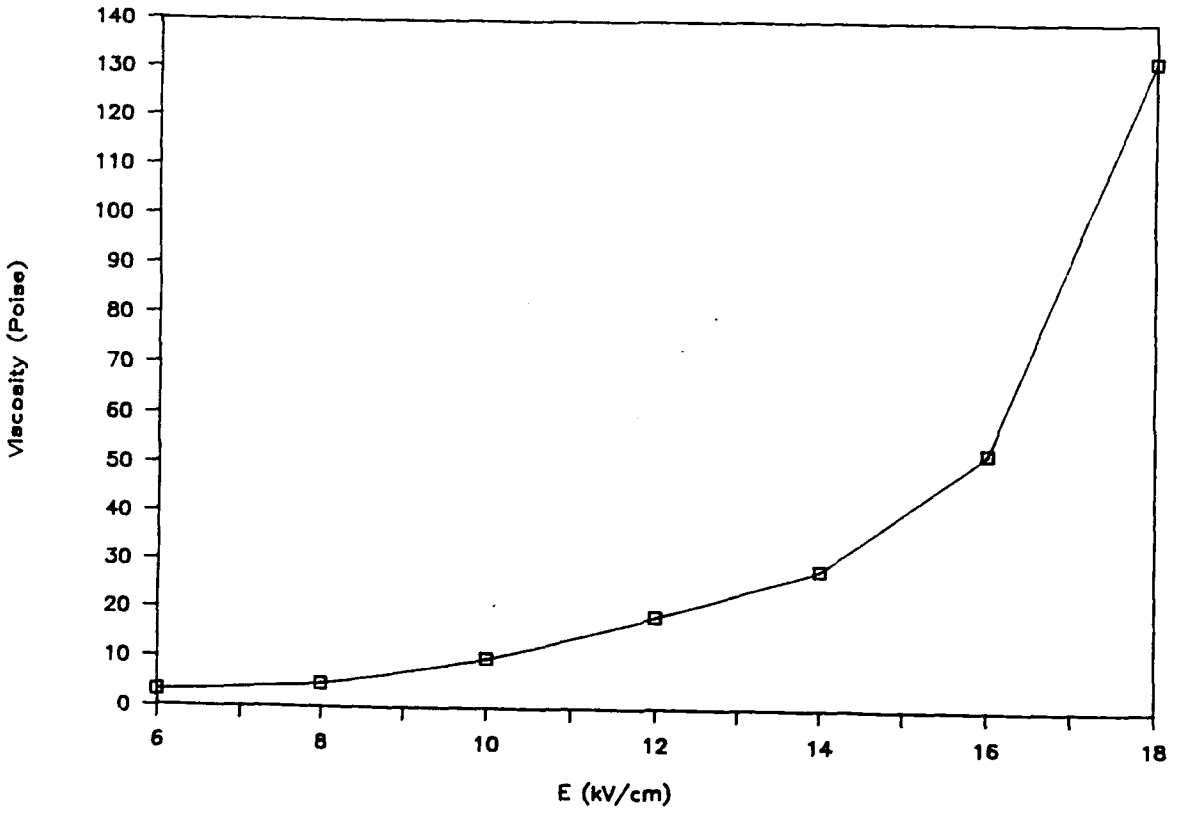

Fig.3. The apparent viscosity as a function of the applied electric field.

4. Structure transitions

We use computer simulations to study a model which has superconducting spheres of radius a in a liquid. The whole system experiences an electric field in the z-direction and a magnetic field in the x-direction. Then the particles have induced electric dipole moment $\vec{p}$ in the z direction and magnetic dipole moment $\vec{m}$ in the x direction.

The electric field induced solidification in our model produces a body-centered tetragonal (bct) lattice with its main axis in the z direction. In a magnetic field, due to the Meissner effect, superconducting spheres obtain a magnetization in the opposite direction to the field. If the system experiences a magnetic field only, we expect that the interaction between these magnetic moments will lead to a solidification similar to the electric field induced solidification. In our model, the solidification induced by a pure magnetic field will have a bct lattice with its main axis in the x direction. Therefore, the structure of the model is determined by the competition between the electrical dipolar interaction and the magnetic dipolar interaction.

Introduce a parameter, $\lambda = m^2/p^2$. We have found three different solid structures.

(a) When $\lambda < 0.544$, the system is a body-centered tetragonal (bct) lattice with three conventional Bravais lattice vectors $2a\hat{z}$, $\sqrt{6}a\hat{x}$, and $\sqrt{6}a\hat{y}$.

(b) When $0.544 < \lambda < 1.838$, the system is a face-centered cubic (fcc) lattice with three conventional Bravais lattice vectors $2\sqrt{2}a\hat{x}$, $2\sqrt{2}a\hat{y}$, and $2\sqrt{2}a\hat{z}$.

(c) When $1.838 < \lambda$, the system changes from the fcc lattice to another bct lattice with three conventional Bravais lattice vectors $2a\hat{x}$, $\sqrt{6}a\hat{y}$, and $\sqrt{6}a\hat{z}$.

These findings are extremely interesting because they are related to the symmetry of space. Further investigation is under way.

5. Order parameters and phase transitions in ER fluids

From the theory of critical phenomenon, it is well known that the order parameters are the key quantities to specify the many-body system in the study of phase transition. The ground state of an induced ER solid is the bct lattice in Fig.1 (a). The reciprocal lattice vectors are $\vec{b}_1 = 2\pi\hat{x}/\sqrt{6}R - \pi\hat{z}/R$, $\vec{b}_2 = 2\pi\hat{y}/\sqrt{6}R - \pi\hat{z}/R$, and $\vec{b}_3 = 2\pi\hat{z}/R$. Three order parameters are, therefore, defined as $\rho_j = \sum_{i=1}^{N} \exp(i\vec{b}_j\vec{r}_i)/N, (j = 1,2,3)$, where N is the total number of particles. Among them, ρ_3 characterizes the formation of chains in the z direction, while ρ_1 and ρ_2 characterize the structure in the x-y plane.

We introduce a dimensionless quantity $\theta = kTd^3\epsilon_f/(\vec{p})^2$ which characterizes the ratio between the thermal energy and the dipolar interaction energy. To

calculate $\bar{\rho}_j$, we apply the Metropolis algorithm. Our simulations take $N = 178$ dielectric particles inside a capacitor with spacing $L = 28a$. In the x and y directions, the system has $360a \times 360a$ and a periodic boundary condition. We start at $\theta = 0$, then increase θ slowly. The state of $\theta = 0$ represents extremely strong electric field which has the ideal bct lattice structure. For each θ, the simulations repeat $1000N = 178000$ Monte Carlo steps. In each step, we pick a particle in the configuration to make a trial move to a position randomly distributed in the space, then calculate the change of dipolar interaction of the system due to the random move, δU_d. If $\delta U_d \leq 0$, we accept the new configuration. If $\delta U_d > 0$, the probability to accept the new configuration is $\exp(-\delta U_d/kT)$. When the new configuration is accepted, we calculate the new ρ_j $(j = 1, 2, 3)$ for statistical average. If the new configur .tion is rejected, the previous configuration is retained and the previous values of ρ_j are counted again in statistical average. Then, the next random trial will be either on the newly accepted configuration or the retained previous configuration. After $1000N$ Monte Carlo steps are completed for one θ, we calculate the average values of ρ_j. Then, we increase θ by 0.01 and repeat the above procedure. The starting configuration at $\theta + 0.01$ is the final configuration at θ. To make sure that our average obtained on the Metropolis sampling is the true canonical ensemble average, we examine the results after $200N$, $400N$, $600N$, $800N$, and $1000N$ Monte Carlo steps and see how they are stabilized. This examination convinces us that the Metropolis sampling is effective.

The absolute values of $\bar{\rho}_j$ are plotted in Fig.4. It is clear that $|\bar{\rho}_1|$ and $|\bar{\rho}_2|$ have almost identical behavior, while $|\bar{\rho}_3|$ is noticeably different. At $\theta = 0$, all the three order parameters equal to unity. As θ increases, $|\bar{\rho}_j|$ (j=1,2,3) remains unity for a while. Then, near $\theta = 0.16$, $|\bar{\rho}_1|$ and $|\bar{\rho}_2|$ drop quickly, while $|\bar{\rho}_3|$ does not drop quickly until θ reaches 0.22. Afterwards, $|\bar{\rho}_1|$ and $|\bar{\rho}_2|$ tend to zero much faster than $|\bar{\rho}_3|$. There are two important quantities, $\theta_1 = 0.28$ and $\theta_2 = 0.67$ When θ reaches θ_1, $|\bar{\rho}_1|$ and $|\bar{\rho}_2|$ are essentially vanishing and their fluctuation after $\theta > \theta_1$ is due to the finite size effect. However, $|\bar{\rho}_3|$ does not vanish until θ reaches θ_2.

The above results indicate three regions of θ. For $0 \leq \theta < \theta_1$, all three $|\bar{\rho}_j|$ are non-vanishing; the ER system is a solid whose ideal structure is the bct lattice.

When $\theta_1 < \theta < \theta_2$, $|\bar{\rho}_1| = |\bar{\rho}_2| = 0$ while $|\bar{\rho}_3| > 0$. Since ρ_3 characterizes the formation of chains in the z direction, the ER system in this state has chains in the field direction, but the distribution of these chains is random, no ordering in the x and y directions. It is clear that this state is similar to an induced nematic liquid crystal, because the chains have orientation in the z direction. As $\theta > \theta_2$, $\bar{\rho}_1 = \bar{\rho}_2 = \bar{\rho}_3 = 0$, the ER system is a fluid with no ordering at all.

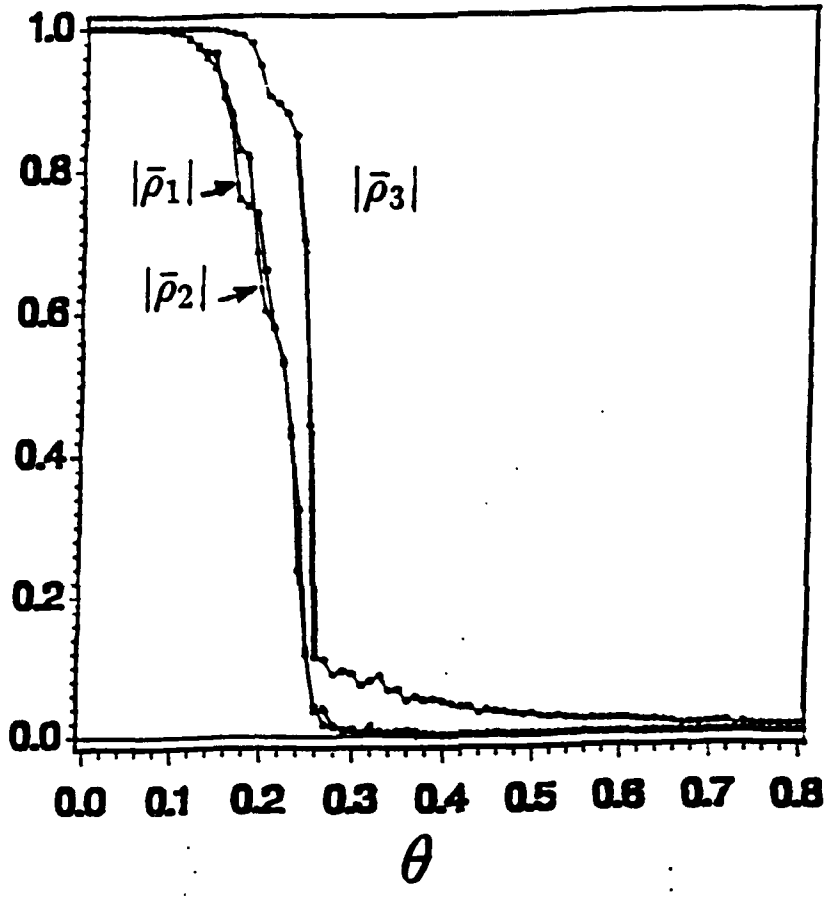

Fig.4. The change of $|\bar{\rho}_1|$, $|\bar{\rho}_2|$, and $|\bar{\rho}_3|$ vs θ. The curves of $|\bar{\rho}_1|$ and $|\bar{\rho}_2|$ are almost identical, while $|\bar{\rho}_3|$ decreases much slower than $|\bar{\rho}_1|$ and $|\bar{\rho}_2|$ as θ increases.

The canonical ensemble average of the dipolar interaction per particle, $\overline{U_d}/N$, is plotted in Fig.5. Though our system is small, $\overline{U_d}/N$ clearly shows a jump as θ crosses θ_1, indicating the first order phase transition from the nematic liquid crystal state to the solid state. Since $\overline{U_d}/N$ is smooth at θ_2 with no jump, the phase transition from the fluid state to the liquid crystal state is of the second order. At $\theta = 0$, $\overline{U}_d/N = -2.71188p^2/(\epsilon_f d^3)$ which is slightly higher than

$-3.050144p^2/(\epsilon_f d^3)$, the value for the infinite bct lattice. This deviation is due to the finite size effect, since a system of 178 particles plus their images is a finite bct lattice with defects and surfaces. We also note that a face-centered cubic lattice of the same small size has dipolar energy $-2.65465p^2/(\epsilon_f d^3)$ per particle, still higher than that of the bct lattice.

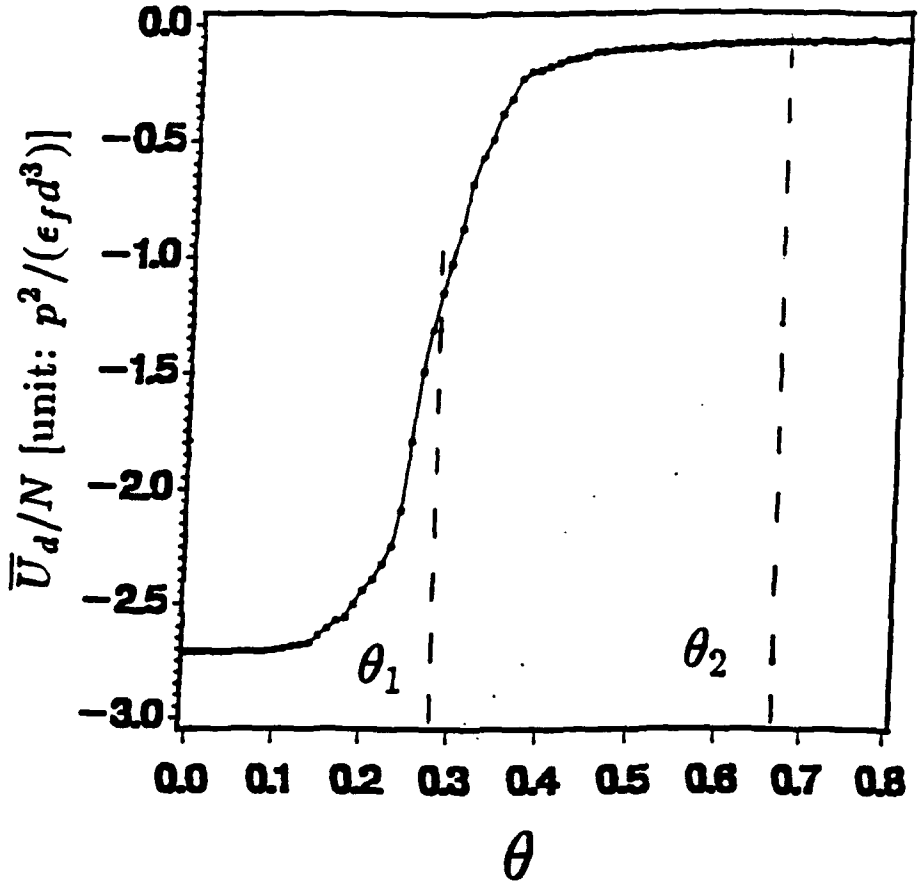

Fig.5. The change of $\overline{U_d}/N$ vs θ. When θ crosses θ_1, $\overline{U_d}/N$ has a jump. There is no jump at θ_2.

Let us estimate the latent heat for the first order phase transition. We define a parameter $\eta = -2\overline{U}_d d^3 \epsilon_f/(Np^2)$. Then the average dipole field is given by $\Delta\vec{E} = \eta\vec{p}/(\epsilon_f d^3)$. Our results indicate that the dipole field and hence η is sensitive to the distribution of dielectric particles [3,10]. Using the Lorentz's self-consistent method, we have the average $\vec{E}_l = \vec{E}/(1-\alpha\eta/8)$, the quantity $\nu = p^2/\epsilon_f = \alpha^2 a^3 E^2 \epsilon_f/(1-\alpha\eta/8)^2$, and the average Coulomb energy per particle $\overline{U}/N = -\frac{1}{2}\alpha a^3 \epsilon_f E^2/(1-\alpha\eta/8)^2$. If η decreases from η_1' to η_1 when θ passes θ_1, the

latent heat per unit volume is given by

$$3\phi\alpha\epsilon_f E^2[(1-\alpha\eta_1'/8)^{-2}-(1-\alpha\eta_1/8)^{-2}]/(8\pi) \tag{3}$$

where $\phi = 4\pi a^3 n/3$ is the volume fraction of the particles in the system. This latent heat is very small for a typical ER fluid. As a rough estimation, we take $\eta_1 \approx 0$ and $\eta_1' \approx 6$, $\phi = 0.4$, $E = 10$ KV/cm, $\epsilon_f = 2.2$ (for petroleum oil), $\alpha = 0.5$, the latent heat is only about 180 erg/cm^3.

We can consider to induce the phase transitions in the ER fluid by two different approaches: (1) At a fixed temperature, increase the applied electric field; (2) at a constant applied electric field, lower the temperature of the ER system. When the ER fluid has a fixed temperature, two critical electric fields are given by

$$E_{ci} = (1-\alpha\eta_i/8)\sqrt{8kT/(\alpha^2\epsilon_f a^3\theta_i)}, \quad (i=1,2), \tag{4}$$

where η_2 is the value of η at θ_2. When $E < E_{c2}$, the ER system is in a liquid state. As $E_{c2} < E < E_{c1}$, the ER system is similar to the induced nematic liquid crystal. As $E_{c1} < E$, the ER system is in the solid state.

When the ER fluid is under a constant electric field, we have two critical temperatures,

$$T_{ci} = \alpha^2\epsilon_f a^3 E^2\theta_i(1-\alpha\eta_i/8)^{-2}/(8k), \quad (i=1,2), \tag{5}$$

if ϵ_f and ϵ_p have little change in the temperature range under our consideration. When $T > T_{c2}$, the ER system is a liquid. When $T_{c2} > T > T_{c1}$, the ER system is similar to nematic crystal state. When $T < T_{c1}$, the ER system is the solid bct lattice.

6. Organizing an International Conference on ER fluids

With the support from ONR and Southern Illinois University at Carbondale (SIUC), we organized an International Conference on ER Fluids on October 15-16, 1991 at SIUC.

The meeting was organized to bring together the experts in this field to explore the state-of-art of this technology, and to disseminate the most recent research developments. Technical sessions included Materials Technology, Physical Mechanisms, Properties, and Applications, together with a poster session. The response from the scientific and engineering community was overwhelmingly positive. The meeting provided a forum for collaboration and interaction of industry and academia, which is required for the success of any emerging technology. Participation from UK, Japan, USSR, China, Germany, France and USA is evidences of the truly international interest in this technology area. It is evident from the presentations that considerable advances have been made in understanding the physics of ER fluids, and that the technology is applied in several components.

The Electrorheological Conference has provided one step to achieve the goal of understanding, controlling and applying ER phenomena.

III. Research in Progress and Work Planned for Next Year

As stated above, our research in last year has clarified several key issues in this field. However, more important questions remain to be solved.

1. Effects of particle size and concentration in ER fluids

An electric field applied to an ER fluid initially induces the formation of particle chains, followed by the coalescence of chains into thick columns, and as a result, the effective viscosity of the fluid increases greatly. The formation of these structures and the strength of the inter-particle forces within them continue to be the subject of theoretical investigations. Our theory predicts that the critical field E_c is inversely proportional to the square root of the particle volume, if everything else remains the same. Therefore, it appears that the bigger the dielectric particles, the stronger the ER effect. There have been, however, few experimental studies of the effects of particle size.

We have begun an extensive set of measurements of the viscosity of an ER fluid as a function of particle size and concentration, and electric field. The main group of measurements utilize the method of falling-ball viscometry, in which the viscosity is calculated from the velocity of a ball falling through the liquid; the velocity is obtained from the time-of-flight passage of the ball through laser beams. These results will be compared with the viscosities inferred from

measurements of the flow resistance through an ER cell in other experiments. At present, the falling-ball viscometer has been constructed and tests on simple fluids of known viscosity have been made to verify that correct results are being obtained. ER fluid measurement will begin shortly.

The measurement of the effects of particle size and concentration on viscosity as described above should be invaluable for developments in both theory and practical devices.

2. Research on cryogenic ER fluids and energetic ER fuels

The development of ER fluids operating at cryogenic temperature, e.g. that of liquid oxygen or liquid nitrogen, poses special problems. When the ER fluid component is a liquified gas, its low density makes it difficult to obtain a uniform suspension of the particles normally used for ER fluids. The particles here must be chosen to have a low density and yet a high dielectric constant as required for a strong ER effect.

We are conducting preliminary experiments in which a polar organic liquid such as ethanol is forced through an atomizer nozzle in a cold chamber, forming small frozen particles. Such particles are adequately suspended in liquid nitrogen. Stable electrodes will need to included in the nozzle to neutralize static charge during particle formation.

We expect that fine frozen ethanol particles in liquid oxygen is an energetic fuel. In addition, this is an ER fuel, or an intelligent fuel, which will show a strong ER effect. We can utilize the ER phenomenon to control its viscosity and flow rate and solidify the fuel.

This research will also be conducted in connection with the study of slurry fuel of liquid oxygen and aluminum powders. Application of the ER phenomenon to solidify the slurry fuel for storage or to control its viscosity is an important part of our research. From our experiment with aluminum powders in oil, the slurry fuel of liquid oxygen and aluminum powders is an ER system. Liquid oxygen has a very low dielectric constant, 1.465. Aluminum powders, though having oxidized films, still have a very high dielectric constant. The only problem here is density mismatch: Aluminum powders are much heavier than liquid oxygen. The frozen ethanol particles will be an ideal additive to the slurry fuel, since they have a

low mass density. We expect that a small amount of fine frozen ethanol particles in the mixture of liquid oxygen and aluminum powders will greatly enhance the ER effect and resolve the problem of density mismatch. In this way, the slurry fuel will become very intelligent ER fuel. We will then examine the change of viscosity and see the condition for solidification.

3. Viscosity and ER valves

We will continue our present study about the viscosity of ER fluids. First, we need to extend our investigation to three-dimensional situation. Second, we want to connect the present issue to the problem of flows in porous media. We have found that the chain shape in two-dimensional ER flow. Experimental results basically agree with the theoretical calculation. The flow structure in three-dimensional space needs to be clarified now. There is a claim that three-dimensional ER flows have layer structure. Each layer is two-dimensional. If this conclusion is always true, the problem would be simplified. However, it seems to doubt whether this claim is true at a high flow rate.

Based on our understanding of the change of viscosity of ER fluids as a function of applied electric field, we will undertake research on ER valves, a device to control liquid fuel flow by the ER phenomenon. This will include search for suitable fuel additives to enhance the ER effect and experimental tests. Dr. Brooks in UK have made several design of ER valves. Among them, the concentric cylinder ER valve shows the best result in tests. His concentric cylinder ER valve is basically the same as our experimental devices for viscosity experiments. Therefore, we will consider to improve our experimental devices for ER valve design.

4. The fluid dynamics and rheology of ER fluids

Fluid dynamics and rheological properties of ER fluids are important and very controversial now. Most groups claim that in the presence of a strong electric field, ER fluids behave like a Bingham plastic with a field dependent excess shear stress over that of the fluid with no field. However, there is also one group claiming that ER fluids in a strong electric field are completely different from a Bingham plastic and there is no yield stress.

Also recently, based on his calculation, Dr. Kraynik claims that thick chains

in ER fluids are even weaker than a single chain. On the other hand, Dr. Conrad stresses that his experiments show that thick chains in ER fluids are much stronger than a single chain.

In order to clarify the issue, we have begun a numerical calculation about shear stress of induced ER solid under a deformation. We have also started a computer simulation, molecular dynamics of polarized particles in an applied electric field. Our preliminary results are consistent with Dr. Conrad's experiments. We hope that our simulations will clarify the above issues.

In near future, after we have some analytical results, we plan to perform some related experiments about fluid dynamics and rheological properties of ER fluids.

5. The ER response in applied a.c. fields

The ER effect in an ac field is important but unclear. We will first extend our theory by replacing the d.c. dielectric constant with the a.c. dielectric constant, $\epsilon = \epsilon_0 + 4\pi i\sigma/\omega$ where ϵ_0 is the d.c. dielectric constant, σ is the conductivity, and ω is the frequency of the a.c. field.

There are only limited experimental data available about the ER response in a.c. field. Therefore, we are considering to perform experiments to investigate the issue, such as solidification, viscosity, and shear stress, etc. It is clear that there are several time scales appearing in the present problem: (i) the time scale for polarization of dielectric particles; (ii) the time scale of ϵ_0/σ; and (iii) the time scale for dielectric particles to form ER structures immediately after an electric field is applied. We have to carefully examine these time scales and clarify their roles in the ER responses.

6. Search for strong ER systems

This will not limit us in search for strong ER materials, such as suitable dielectric particles and base liquids. We are also considering how the structure of an applied electric field affects the strength of ER fluids.

We have found that the ideal structure of ER fluids in a uniform parallel electric field is a body-centered tetragonal lattice. However, this may not be the best structure for an induced ER solid. Other structures may produce a better mechanic properties for the ER solid. Therefore, there are more to be learned

about the relationship between the structure of ER fluids and the structure of applied electric field. If the applied electric field is not parallel, what would be the ideal structure for ER fluids? This is not an easy task. We plan to study it by computer simulations. After understanding the relationship between the structure of ER fluids and the structure of applied electric field, we will seek the optimal structure of electric field to yield a strong ER system. For example, if the induced ER solid has a structure similar to polymer chains, the strength of the ER solid is greatly enhanced. Then, what kind of applied electric field will produce polymer-like ER solid? This is an "inverse" problem. We will first select a polymer-like structure which has a strong yield stress, then go back and see what is the necessary applied electric field to produce this structure. After we find a way to produce polymer-like ER solid, we will study its physical properties.

IV. Invited Papers Presented at Conference

1. R. Tao, "Order Parameters and Phase Transition in ER Fluids", invited talk at the International Conference on ER Fluids, held on October 15-16, 1992, at Southern Illinois University at Carbondale.

2. T. Chen, R. N. Zitter, and R. Tao, "Crystalline Structure of an Electrorheological Fluid Determined by Laser Diffraction", invited talk at the International Conference on ER Fluids, held on October 15-16, 1992, at Southern Illinois University at Carbondale.

3. R. Tao, "Ground State of Electrorheological (ER) Fluids", invited talk at the American Physical Society 1992 March Meeting, 16-20 March 1992, Indianapolis, Indiana. The abstract is published in Bulletin of the American Physical Society, V.37, N.1, p570 (1992).

4. R. Tao, "Phase Transition and Order parameters in ER Fluids", invited talk at the 2nd Minsk International Heat and Mass Transfer Forum, May 19-23, 1992, Minsk, Beloruss.

V. Invited Seminars

1. R. Tao, "Structures and Phase Transition in Electrorheological Fluids", Department of Physics and Department of Material Science, Michigan State University, East Lansing, MI, April 23, 1992.

2. R. Tao, "Electric Field Induced Solidification in a Low Gravity Environment

and Electrorheological Fluids", Tampere University of Technology, Finland, May 15, 1992.

VI. Papers at Professional Society

1. R. Tao, "Electric Field Induced Solidification in the Gravity-Free Environment", American Physical Society March Meeting, 16-20 March 1992, Indianapolis, Indiana.
2. G. L. Gulley and R. Tao, "Static Shear Stress of Induced Electrorheological Solids", American Physical Society March Meeting, 16-20 March 1992, Indianapolis, Indiana.
3. T. Chen, R. N. Zitter, and R. Tao, "Laser Diffraction Study of Crystalline Structure in an Electrorheological Fluid", American Physical Society March Meeting, 16-20 March 1992, Indianapolis, Indiana.
4. X. Zhang, T. Chen, R. N. Zitter, and R. Tao, "Influence of Electrode Roughness on the Apparent Viscosity of an Electrorheological Fluid", American Physical Society March Meeting, 16-20 March 1992, Indianapolis, Indiana.

VII. Publications with Acknowledgement to ONR

1. R. Tao and J. M. Sun, "Ground State of Electrorheological Fluids from Monte Carlo Simulations", Phys. Rev. A. (Rapid Communication), **44**, R6181-R6184 (1991).
2. T. Chen, R. N. Zitter, and R. Tao, "Laser Diffraction Determination of the Crystalline Structure of and Electrorheological Fluid", Phys. Rev. Lett. **68**, 2555-2558 (1992).
3. R. Tao, "Order Parameters and Phase Transition in ER Fluids", in ***Electrorheological Fluids***, edited by R. Tao (World Scientific Publishing, Singapore, 1992) pp 1-14.
4. T. Chen, R. N. Zitter, and R. Tao, "Crystalline Structure of an Electrorheological Fluid Determined by Laser Diffraction", in ***Electrorheological Fluids***, edited by R. Tao (World Scientific Publishing, Singapore, 1992) pp 15-20.
5. A book, ***Electrorheological Fluids***, (Proceedings of the International Conference on ER Fluids, Oct. 15-16, 1991 at Southern Illinois University, Carbondale, Illinois) was edited by R. Tao (World Scientific Publishing, Singapore, 1992)